Journal of Earth Science and Engineering 2 (2012) 496-513

Mapping Seismic Vulnerability and Risk of Cities: The MASSIVE Project

Charalampos Kontoes[1], Themistoklis Herekakis[1], Emmanouela Ieronymidi[1], Iphigenia Keramitsoglou[1], Anna Fokaefs[2], Gerasimos A. Papadopoulos[2], Sideris Paralikidis[3], Dorothea Aifantopoulou[3], Anna Maria Deflorio[4], Daniela Iasillo[4] and Chris T. Kiranoudis[5]

1. Institute for Astronomy, Astrophysics, Space Applications, and Remote Sensing, National Observatory of Athens, Athens GR 152-36, Greece

2. Institute of Geodynamics, National Observatory of Athens, Athens GR 118-10, Greece

3. Geoapikonisis SA, Athens GR 11-524, Greece

4. Planetek Italia Srl, Bari I 70-123, Italy

5. Department of Process Analysis and Plant Design, School of Chemical Engineering, National Technical University of Athens, Athens 157-80, Greece

Received: July 29, 2012 / Accepted: August 10, 2012 / Published: August 20, 2012.

Abstract: MASSIVE (mapping seismic vulnerability and risk of cities) is a GIS-based earthquake preparedness system that was developed under the European Union Civil Protection Mechanism project (GA No. 070401/2009/540429/SUB/A4), in order to provide civil protection authorities with accurate, and easily transferable tools for generating up-to-date maps of seismic hazard, seismic vulnerability and seismic risk of buildings, at the scale of the single building block. In addition, MASSIVE developed and ran state-of-the-art models to assess the risk for population evacuation in dense urban agglomerations given an earthquake event. The MASSIVE methodology was designed, implemented and validated considering two European pilot sites, heavily struck by recent earthquakes, which are the western part of the Larger Metropolitan Area of Athens (GR), and the city of L' Aquila in the Abruzzo Region (IT). The validation of the results using past earthquake records shows that the performance of MASSIVE is prosperous, achieving a correlation between the modeled and the on-site measured PGAs (peak ground accelerations) higher than 0.75, while the correlation between the on-site reported building damages and the ones predicted by the MASSIVE system has been of the order of 0.80.

Key words: MASSIVE, seismic risk, damage assessment, building vulnerability, evacuation risk.

1. Introduction

Seismic risk assessment is a comprehensive procedure, and consists a fundamental step in acting towards the earthquake disaster prevention. Damages due to seismic events in the last decades, particularly in cities with dense urban fabric, have raised the interest of emergency planners in estimating the seismic risk associated with future earthquakes. Thus, during the last years, several models were developed for assessing the vulnerability of buildings and to estimate the expected earthquake damages. The methods developed can be either empirical, such as the ones based on "damage-motion relationships" or analytical/mechanical based on the fragility curves of buildings, or hybrid methods [1-4]. GIS-based models for seismic hazard and damage estimations have been deployed in various studies and relevant projects in the past. Specific examples include: (2) HAZUS-HAzards in the US [5]; (2) RISK-UE project [6]; (3) RADIUS-Risk assessment tools for diagnosis

Corresponding author: Charalampos Kontoes, Ph.D., research director, main research fields: remote sensing of environment, natural disaster emergency response, safety and security of citizens. E-mail: kontoes@noa.gr.

of urban areas against disasters [7]; (4) SEISMOCARE [8]; (5) EPEDAT (early post-earthquake damage assessment tool) [9]; (6) VULNERALP project [10]; (7) LESSLOSS project [11] and (8) Risk Link® [12].

RISK-UE, HAZUS and RADIUS produce seismic scenarios and estimations of risks and vulnerabilities in the case of a plausible earthquake which may affect specific cities in the geographic context of the European Union, and the United States, respectively. VULNERALP focuses in zones with moderate-to-low seismic hazard, and its pilot sites are constrained in the French territory. The EPEDAT tool employs applicable ground motion and soil amplification models to estimate the expected intensity patterns in the area of interest which, combined with an aggregate listing of buildings and lifelines, provides estimates of the damages and casualties for the impacted area. Seismic assessments of existing structures, earthquake disaster scenario prediction and loss modeling over urban areas have been also studied in the frame of the LESSLOSS project. Risk Link® finally is a commercial software package which allows for catastrophe risk management and provides assessment of property damage and uncertainty around associated losses.

Some of the proposed models in these studies are site specific while others can be potentially transferred to new sites, but there is need for special adaptations in order to meet the specificities of the target areas, with the most demanding ones concerning the definition and classification of building typologies. This requires detailed building reporting and analysis of their structural aspects at the level of the building block over the study area.

The study presented in this paper that is the outcome of the EC-DG ECHO project MASSIVE (http://massive.eu-project-sites.com/) proposes an alternative approach to overcome such restrictions. Although MASSIVE similarly to other systems accounts for building typologies and their structural characteristics, and in addition to that, if detailed building data are not available, MASSIVE allows using a simplified approach which accounts only for the oldness of the buildings in respect to the National Anti-seismic Building Codes/Regulations applied over the years in the study area. Another important aspect of MASSIVE is the large mapping scale it refers to for assessing the vulnerability and the damages of the buildings. It is also interesting to note that MASSIVE relies on a minimum set of easily derived information layers, exploiting widely accessible and commonly used data at any geographic area. Therefore, the MASSIVE concept builds upon a generic and transferable methodology. For this, a specifically developed set of GIS tools has been implemented. It enabled the users to easily derive seismic hazard, and build vulnerability assessments, and also predict the expected building damages for any user defined earthquake scenario.

Last but not least is the capability of MASSIVE to assess one of the most critical aspects during an earthquake occurrence, which is the risk for uncontrolled population evacuation. This task is complex because of the high degree of uncertainty in the spatial impact of the earthquake event, as there are numerous points affected by the incident and at different intensities. This means that for each possible incident, different evacuation zones are defined, which are not known until the time of the incident. Therefore, tools designed for the evacuation process during other hazardous situations, for which the evacuation zones are determined in advance (e.g. airports, harbors, industrial plants, critical buildings), are not applicable to solve the earthquake uncontrolled population evacuation problem [13-15]. In this sense MASSIVE models the worst possible scenario for evacuation and classifies each area in terms of evacuation difficulty. For this, MASSIVE considers the demographic characteristics and the real transportation network capabilities that may lead to significant problems in evacuation during a seismic event. As a result, the key

effort in MASSIVE is to predetermine relatively small areas or neighborhoods that may be difficult to evacuate.

The remainder of the paper is structured as follows. Section 2 introduces the rationale behind the MASSIVE project. Section 3 provides an overview of the techniques used in MASSIVE in order to develop the damage assessment and population's uncontrolled evacuation models. Section 4 provides an overview of the MASSIVE geo-information system. Section 5 presents the assessments outcomes of MASSIVE regarding the (1) seismic hazard, (2) building vulnerability, (3) building damages, and (4) risk for uncontrolled evacuation over the two pilot sites analyzed in the framework of the study for specific earthquake scenarios. A validation of the results is presented in Section 6, while Sections 7 and 8 arisen from the MASSIVE system applicability are presented in the homonymous sections.

2. The MASSIVE EC Project

2.1 MASSIVE Scope

MASSIVE is a project supported by the EU Civil Protection Mechanism (GA No. 070401/2009/540429/SUB/A4, http://www.massive.eu-project-sites.com/). The focus of MASSIVE is to provide stakeholders with a methodology for reliable and up-to-date mapping of damages caused by strong earthquakes over urban agglomerations. Stakeholders may include local and central civil protection authorities, decision planners and decision makers, fire brigades and rescue teams as well as the insurance industry. Therefore, in the framework of MASSIVE, the term seismic risk is approached by estimating the damage level at large scale coupled with state-of-the-art uncontrolled population evacuation modeling. From the civil protection point of view, MASSIVE is a prevention tool that enables managers and authorities to prepare for managing earthquake incidences in urban areas.

2.2 Test Areas

Two European pilot sites were selected in the framework of MASSIVE, which were heavily struck by strong earthquakes in the recent past. The first is the western side of the larger metropolitan area of Athens, capital city of Greece (GR), that was hit by the lethal earthquake of September 7, 1999 (magnitude M = 5.9) causing 143 human victims. Actually within this area nine municipalities were appropriately selected to constitute the test site for MASSIVE. Seven out of nine municipalities are located close to the epicenter area of the earthquake. The other two municipalities are situated further from the epicenter and they were also included in the analysis to assess the performance of the proposed methodology both in near-field and far-field areas.

The second test site is the city of L'Aquila in the Abruzzo Region of Italy (IT) that was struck by the lethal earthquake (M = 6.3), of April 6, 2009, causing 310 human victims. The test area for MASSIVE project has included an area of about 160 km^2 around the L'Aquila municipality. The two test sites are illustrated in Fig. 1.

3. Methodology

3.1 Damage Assessment

There is high need in the metropolitan cities to study the seismic risk, since the seismic hazard although might be low, the resulted risk expressed in terms of damages and human casualties can be high due to the high average density of built up areas, population and economic activities. A characteristic example is the metropolitan area of Athens that is of low seismic hazard as compared to other seismogenic zones of Greece, but occupying the top position from the risk point of view [16]. This was verified with the occurrence of the September 7, 1999 earthquake, which although was of moderate physical size (magnitude M = 5.9), it caused the most costly impact ever reported in Greece, estimated as high as 3 billion USD.

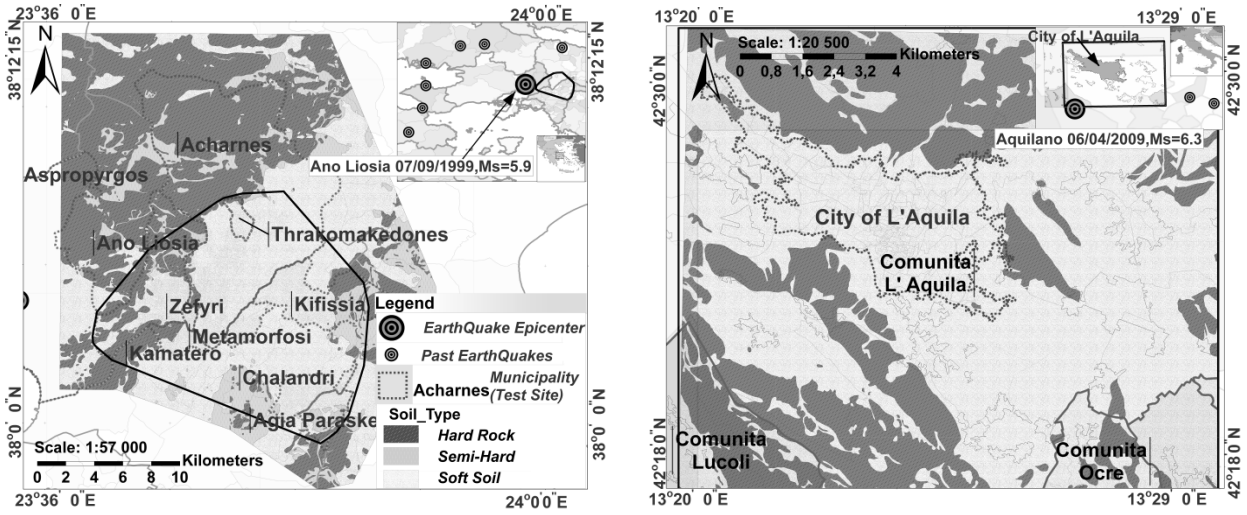

(a) Athens test site (b) L'Aquila test site

Fig. 1 The two test sites studied in the framework of MASSIVE: (a) the most densely occupied part of the nine municipalities in the larger metropolitan area of Athens (indicated by the envelop polygon in black), and (b) the city of L'Aquila and its surrounding area of approximately 160 km^2.

In the framework of MASSIVE, the main priority in the methodology design was to develop a generic model for the rapid and low-cost assessment of the expected risk from future earthquakes. For this a quantitative approach of risk (R), was considered, as the convolution of three critical parameters: hazard (H), vulnerability (VU), and value exposed to hazard (VA).

$$R = H \times VU \times VA \quad (1)$$

From Eq. (1), it comes out that the expected damage, $D(A)$, in a given area A is a function of H and VU, that is

$$D(A) = H \times VU \quad (2)$$

For the purposes of the study the parameter value at risk was not considered, and the damage in buildings has been chosen as the measure of the seismic risk.

In relatively large areas, such as the metropolitan area of Athens but also in smaller cities like L'Aquila, the hazard and vulnerability parameters may vary geographically within the area. This implies that the expected building damages also vary over the study area.

Let authors suppose that an area A is subdivided in n adjacent subareas, Ai, where i =1, 2, …, n. These subareas can be municipalities, communities, neighborhoods or districts, or the building blocks as is the case for MASSIVE. The purpose is to estimate the expected lateral variation of damage within the area A by calculating the expected damages, $D(Ai)$, in each one of the subareas determined. Then,

$$D(A_i) = H_i \times VU_i \quad (3)$$

The parameter H_i is the seismic hazard expressed by the parameter PGA (peak ground acceleration), as described hereinafter, and VU_i is the vulnerability in the subarea i. The term vulnerability may apply to different attributes such as population, property or buildings. In this study the vulnerability of buildings was considered, given this parameter was possible to quantify. In the remaining of this section the methodology for estimating the hazard and the building vulnerability is described.

Seismic hazard is a description only of the natural phenomenon and, therefore, it is a function of geophysical and geological parameters, such as the earthquake source properties and the focal parameters of the earthquake, the attenuation of the seismic waves from the source to the target area, and the local site effects (e.g. geology) in the target area. As mentioned the most appropriate expression of the strong ground

motion to be used in the study was considered the PGA. For a particular site the PGA is dependent on the earthquake's magnitude, the distance from the epicenter of the earthquake, the local site conditions and the pattern of seismic energy radiation moving away from the seismic source, i.e. the type of seismic fault activated. Empirical site-specific attenuation laws for the PGA based on past earthquake records are in extensive use in many countries, with the aim to provide quantitative estimations of ground shaking given a specific earthquake scenario. Such general use empirical functions have been used in the two pilot sites of the study. As test earthquakes, it selected the ones of September 7, 1999, for Athens, and April 6, 2009, for L'Aquila. As regards the Athens site, it has been used the most recent and well-tested attenuation law of PGA (expressed in cm/sec^2) that has been developed, tested and published by Skarlatoudis et al. [17]. This law is applicable to entire Greece, and is as follows:

$$\log \text{PGA} = 0.86 + 0.45M - 1.27 \log (d^2 + h^2)^{½} + 0.10F + 0.06S \ (\pm 0.286) \quad (4)$$

and

$$\log \text{PGA} = 1.07 + 0.45M - 1.35 \log (d + 6) + 0.09F + 0.06S \ (\pm 0.286) \quad (5)$$

where M = earthquake magnitude, d = epicentral distance (in km), h = hypocentral distance (km), F is a factor denoting the type of the seismic fault, and S is a factor taking the value of 0 for hard rock, 1 for semi-hard rock or 2 for soft soils. Eq. (4) is applicable for near-field conditions, that is for short epicentral distances (d < 30 km) of shallow earthquakes (h < 50 km), and for intermediate-depth earthquakes where the hypocentral depth is considerable (h > 50 km). On the other hand, Eq. (5) is applicable for the far-field conditions, which is for long epicentral distances (d > 30 km). In far-field conditions one may expect that the focal parameters of the earthquake do not affect PGA significantly due to the large distance. Then, it is expected that PGA is mainly controlled by local site effects as geology.

A similar empirical formula has been suggested by Sabetta et al. [18] for Italy, and was used in the Abruzzo Region over the test site of L'Aquila, with the PGA parameter expressed in g (1 g = 9.81 m/sec^2):

$$\text{Log PGA} = -1.562 + 0.306\, M - \log(d^2 + 5.82)^{1/2} + 0.169\, S \quad (6)$$

where, M = earthquake magnitude, d is the closest distance to the surface projection of the fault rupture (in km), which for practical reasons was taken as equal to the epicentral distance (in km), and S is a variable taking the value of 1 for shallow and deep alluvium sites or 0 otherwise. Practically, for soft soil S = 1 and for hard soil S = 0. Eq. (6) is applicable for $4.5 \le M \le 6.8$ and $d \le 100$ km.

As regards the building vulnerability, it describes the degree of weakness of the built environment. Building vulnerability depends on many different parameters which are hard to quantify. Critical parameters however are the oldness of buildings and the technology used for their construction, coupled with the application of a building code or not. In the presence of a building code the building's time history is also of great interest. In view of these assumptions the approach proposed and tested in large seismogenic zones of Greece by Papadopoulos et al. [16] has been also adopted for the purposes of the study. In this sense, and given that detailed building structural data are not available at building block level over the two test-sites, the oldness of buildings has been chosen to be the main feature to measure the vulnerability parameter. The ranking of buildings' vulnerability in time is determined by the history of the Anti-seismic Building Codes applied over the two test areas. Following this approach, the oldness of buildings for the test-site of Athens was quantified by the coefficient Σ, defined as,

$$\Sigma = a + 0.5b + 0.3c \quad (7)$$

where, a is the number of buildings constructed before 1965, b is the number of buildings constructed after 1965 and before 1996, and c is the number of buildings constructed from 1996 to 2000 inclusive. The selection of these three time periods was based on the dates of critical changes in the anti-seismic

building codes in Greece. More precisely, the First National Anti-seismic Building Code was put in force by law on 1959 while the New Anti-seismic Building Code on 1992. The year 1965 was considered as a time limit instead of 1959, allowing for some years for actual application of the First National Anti-seismic Building Code. Similarly, the New Anti-seismic Building Code of 1992 code was put in actual application by the end of 1995 and, therefore, 1996 was selected as a time limit. Then, the numbers *a*, *b*, *c* introduced in Eq. (7) could be easily determined from the available statistical building data, the latter recorded in the official national census conducted over the years by the Hellenic Statistical Authority.

In Italy, the critical changes in the Anti-seismic Building Code were marked by the gradual introduction of the Anti-seismic Code at national level between 1981 and 1984, and the general revision of 2003. However, after 2001 there is a lack of available statistical building data based on national census. Subsequently, Eq. (5) was modified for the L'Aquila test-site by assuming *a* as the factor referring to the number of buildings constructed before 1985 and *b* the number of buildings constructed during or after 1985 until 2001. Based on this authors get $c = 0$, for Italy.

Having obtained quantitative expressions for both the seismic hazard and the building vulnerability at *Ai* subareas, each corresponding to a single building block, building damages were computed from Eq. (1). Normalized damage values were then calculated by scaling the returned assessments of Eq. (1) in the range of 1-10. Relative damage values were also calculated for each studied seismic event, by dividing the absolute damage values obtained with the minimum damage value recorded over the study area.

Apart from the resulted damages (normalized/relative) of Eq. (1), another independent parameter that was also calculated, as it provides significant insights to the expected destructions in a particular subarea *Ai*, has been the so-called macro-seismic intensity parameter *I*, which is derived as a function of PGA, such as:

$$\text{Log PGA} = f(I) \quad (8)$$

where, *I* is expressed in the 12-grade Mercalli-Sieberg scale. However, it is worth noting that such expressions suffer from the large uncertainties involved. On the other hand, they are in use only if not high accuracy is expected for the results. For Greece, the empirical relation proposed by Koliopoulos et al. [19] has been applied as:

$$\log \text{PGA} = 0.33I + 0.07 \quad (9)$$

where PGA is measured in cm/sec^2. A similar approach was also applied for L'Aquila test site by using the following expression suggested by Faenza et al. [20]:

$$I = 1.68\ (\pm 0.22) + 2.58\ (\pm 0.14) \log \text{PGA} \quad (10)$$

3.2 Uncontrolled Evacuation of Population

In many seismic events, large urban areas need to be evacuated. In most of these cases, the evacuation process cannot be sufficiently controlled by rescue services, due to the lack of time needed and the unpredictable human behavior at the moment. This can result to accidents which complicate the evacuation process even further, especially in locations where the transportation capacity is limited. There have been reported events, where the injuries or even deaths caused during the evacuation process are significantly larger compared to the ones caused by the earthquake alone [21-24]. The best option in determining risk during uncontrolled evacuation of urban areas is to be able to identify network and demographic characteristics on real transportation networks which may lead to significant problems in evacuation during a seismic event. As a result the key effort is to identify small areas or neighborhoods that may be difficult to evacuate. More specifically, the optimization problem is based on a model that computes for each area the worst possible scenario as far as the ratio of population to exceed network capacity is concerned. Then, that area is classified as to the degree to which evacuation difficulty exists. By applying the model numerous times across the

network and classifying each local area as to evacuation difficulty, a map of evacuation vulnerability can emerge. In this study, the modeling approach of Cova et al. [25] is adopted. Since the difficulty involved in evacuation is inextricably tied to the definition of the neighborhood, then the problem of neighborhood evacuation analysis includes identifying the critical size and shape of the neighborhood in question. Thus, defining the exact boundaries of the neighborhood is part of the evacuation risk mapping problem. According to this analysis, the ratio of population evacuated to the number of lanes leading out of the evacuated neighborhood (bulk lane demand—BLD) is of utmost importance to identify the risk of uncontrolled evacuation. The BLD value for a neighborhood is a simple estimate of the number of vehicles per lane that must evacuate. The methodology relies on the assumption that no accidents occur, that all inhabitants would either drive or ride a vehicle, and that the critical transportation element is the outbound road capacity of the neighborhood. If the BLD values are low, then it is theoretically possible to make a speedy clearance of the neighborhood. If the BLD values are large, this might signal a potential difficulty to evacuate the area, especially if the required time for this is too large in comparison to the time of civil protection response actions. This index is an estimate of the evacuation risk. The larger the values are, the greater the time that is required to clear a neighborhood. The major constraint is that the neighborhoods are not defined in advance. Nevertheless, since the BLD values can be easily calculated for a very large number of possible neighborhood definitions, this will allow authors to actually search for the critical neighborhood. The problem of finding the critical neighborhood of a node in a network is an optimization problem and can be rigorously described as: Given a node of interest, called an anchor node, identify a critical neighborhood of connected nodes and arcs about that anchor node which corresponds to the highest BLD value (Critical Cluster Problem—CCP). CCP is an NP-hard problem in nature, so advanced meta-heuristics were employed to solve it for the case studies of MASSIVE. This is illustrated in Fig. 2. Two datasets of geographic information were integrated to perform a case-study: road network (including number of lanes in each direction) and population. The model was developed in a way that data preparation is minimal. The most involved step was transferring the population from the census data blocks to the nodes of the mathematical network. In authors' case, each population polygon node contributed an equally split fraction of the polygon population to the closest network node.

4. MASSIVE Geo-information System Design and Implementation

4.1 Input Data Set

The actual application of the methodology described in the previous sections was implemented in a GIS system, which accommodates a user interface, an adequate environment for hosting the models and the tools to run, and the data base component. For both test sites the appropriate data layers were processed and integrated in the data base as vector layers following the modeling requirements of MASSIVE. The data layers included: (1) the road network; (2) the city blocks geometry with the attributed census information (source: Hellenic Statistical Authority, census data of year 2000, and Italian National Institute of Statistics, census data of year 2001); (3) the earthquake epicenters and the seismic faults parameters for the two test sites (source: national observatory of Athens-Institute of Geodynamics, year: 2010), and (4) the geology maps (source: Institute of Geology and Mineral Exploration for Athens, and Regione Abruzzo for L'Aquila).

4.2 GIS Implementation

The design of the GIS system shown in Fig. 3 assures optimized functionality and robust model

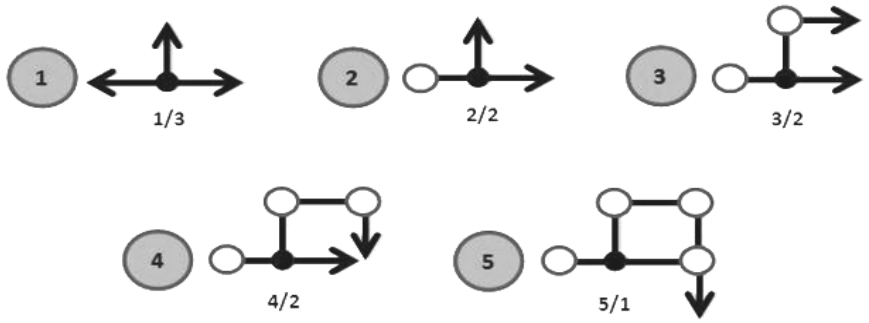

Fig. 2 A critical neighborhood of connected nodes and arcs. The ratio of nodes over exits denotes the difficulty to evacuate the neighborhood (low in example 1 and high in example 5).

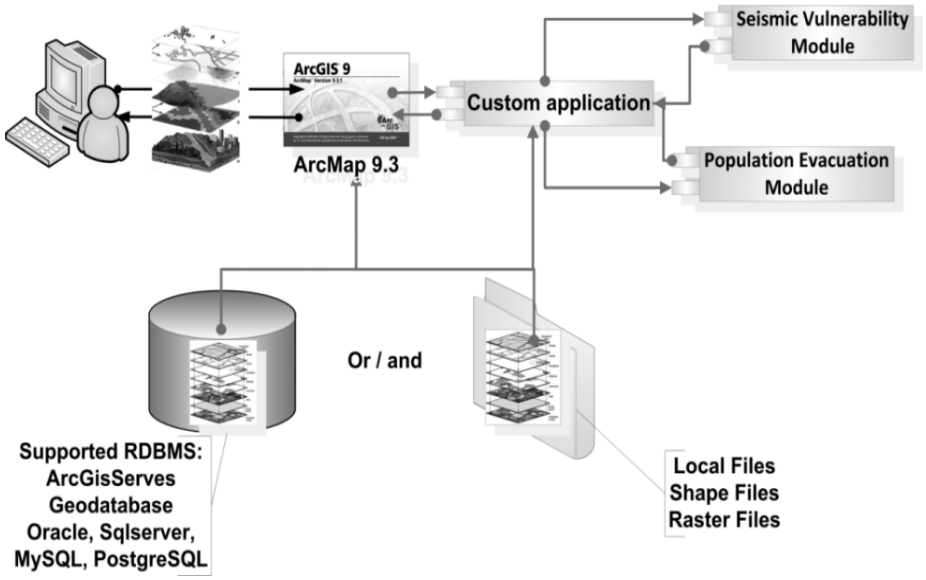

Fig. 3 The MASSIVE GIS system architecture.

handling. The GIS system has been regarded as a custom add-in module for the ArcGIS ArcMap GIS software version 9.3.1 and greater. The user interface of the MASSIVE custom add-in modules consists of (1) the MASSIVE risk toolbar, and (2) the MASSIVE evacuation toolbar. The great advantage for emergency planning is that within the custom add-in module, it is possible to insert new earthquake scenarios, select the area for the models to run, calculate the seismic risk parameters, and assess the population evacuation risk for any part of the road network and the city. The final outputs are thematic maps depicting the results of the MASSIVE models (seismic and evacuation risks) as shown in the following section.

The flowchart of Fig. 4 indicates the processing steps implemented by the MASSIVE GIS system on the basis of the aforementioned methodology.

5. Results

5.1 Earthquakes Scenarios Applied over the Athens and L'Aquila Test Sites

The September 7, 1999 Athens earthquake was generated in a WNW-ESE trending normal fault, dipping to SW [26-29], the so-called Filifault. The epicenter was located approximately 17 km to the northwest of the historical center of Athens, in a sparsely populated area between the urban area of Acharnes and the Mount Parnitha National Park to the north of Acharnes (Fig. 1). The proximity to the Athens Metropolitan Area resulted in widespread

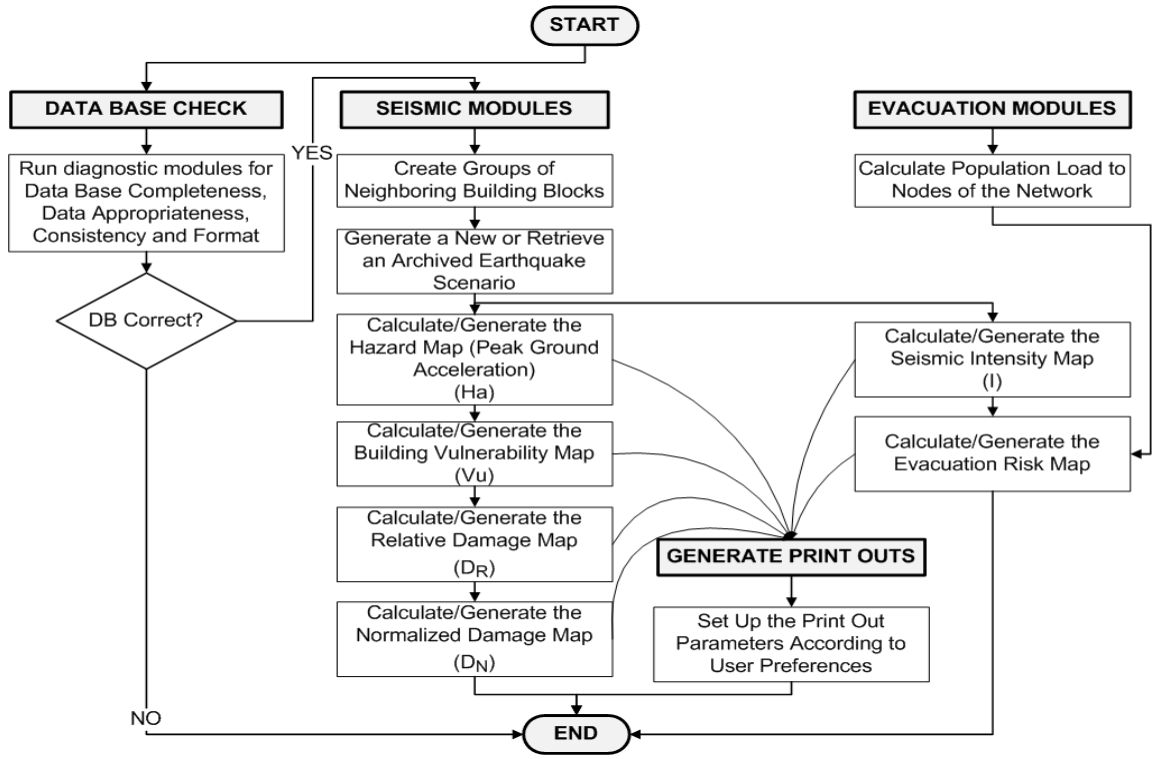

Fig. 4 The workflow implemented in MASSIVE GIS system.

structural damages, mainly to the nearby municipalities of AnoLiossia, Acharnes, Fyli and Thrakomakedones as well as to the northern Athenian suburbs of Kifissia, Metamorfosi, Kamatero and NeaPhiladelphia. The highest recorded PGAvalue from locally deployed seismographs was of 0.3 g at a distance of about 15 km away from the epicenter.

On the other hand the earthquake of April 6, 2009 in the city of L'Aquila was generated from the activation of the 15-km-long normal fault of Paganica, striking about NW-SE and dipping SW (Fig. 1).

5.2 Seismic Hazard Results

Running the 1999 Athens earthquake scenario in MASSIVE, it was observed that the modeled values of PGA vary spatially over the test area ranging from 53.7 cm/sec^2 to 219.1 cm/sec^2. The geographical distribution of PGA is illustrated in Fig. 5a. As it can be seen, the strongest PGA has dominated the southwestern side of the area. This result is quite reasonable given that this area is the closest to the earthquake source. Also it is obvious in Fig. 5a that many local changes in the obtained PGA values are attributed to the local site effects, namely the differences in the soil types denoted as soft and hard soils respectively. As one may expect, the PGA gradually attenuates away from the earthquake source that is towards northeast. In this sense the pattern for the PGA distribution is quite reasonable being controlled mainly by the epicentral distance and the soil effects. As it concerns the run of the April 6, 2009 L'Aquila earthquake scenario, the calculated PGA parameter varied between 129.7 cm/sec^2 and 572.0 cm/sec^2. The corresponding geographical distribution of the modeled PGA is illustrated in Fig. 5b. The pattern of the PGA geographical distribution shows that the highest values have been returned to the areas which are closer to the earthquake source, and gradually attenuated away from the source towards northeast implying once more that PGA is controlled primarily by the epicenter distance as well as the soil conditions.

5.3 Buildings Vulnerability

The spatial distribution of buildings vulnerability for the test site of Athens, as expressed by the Σ coefficient, is illustrated in Fig. 5c. It should be taken into account that by definition the higher the Σ coefficient, the higher the relative oldness of buildings and, therefore, the higher the vulnerability. Fig. 5c shows that the vulnerability is more or less homogeneously distributed in the largest part of the area examined. However, some weaker spots with strong vulnerability appear in the central and east sides of the test area.

This is the result of the aged building typologies existing at those areas, as it can be easily illustrated in the Google Earth images of Fig. 5c. Similarly Fig. 5d illustrates the building vulnerability obtained over the L'Aquila study area. Here the main feature is that most of the building stock in L'Aquila is characterized by high vulnerability, which is obvious given that L'Aquila is a medieval city. This is a clear reflection of the oldness of the majority of the buildings, many of which can be considered as historical and monumental buildings.

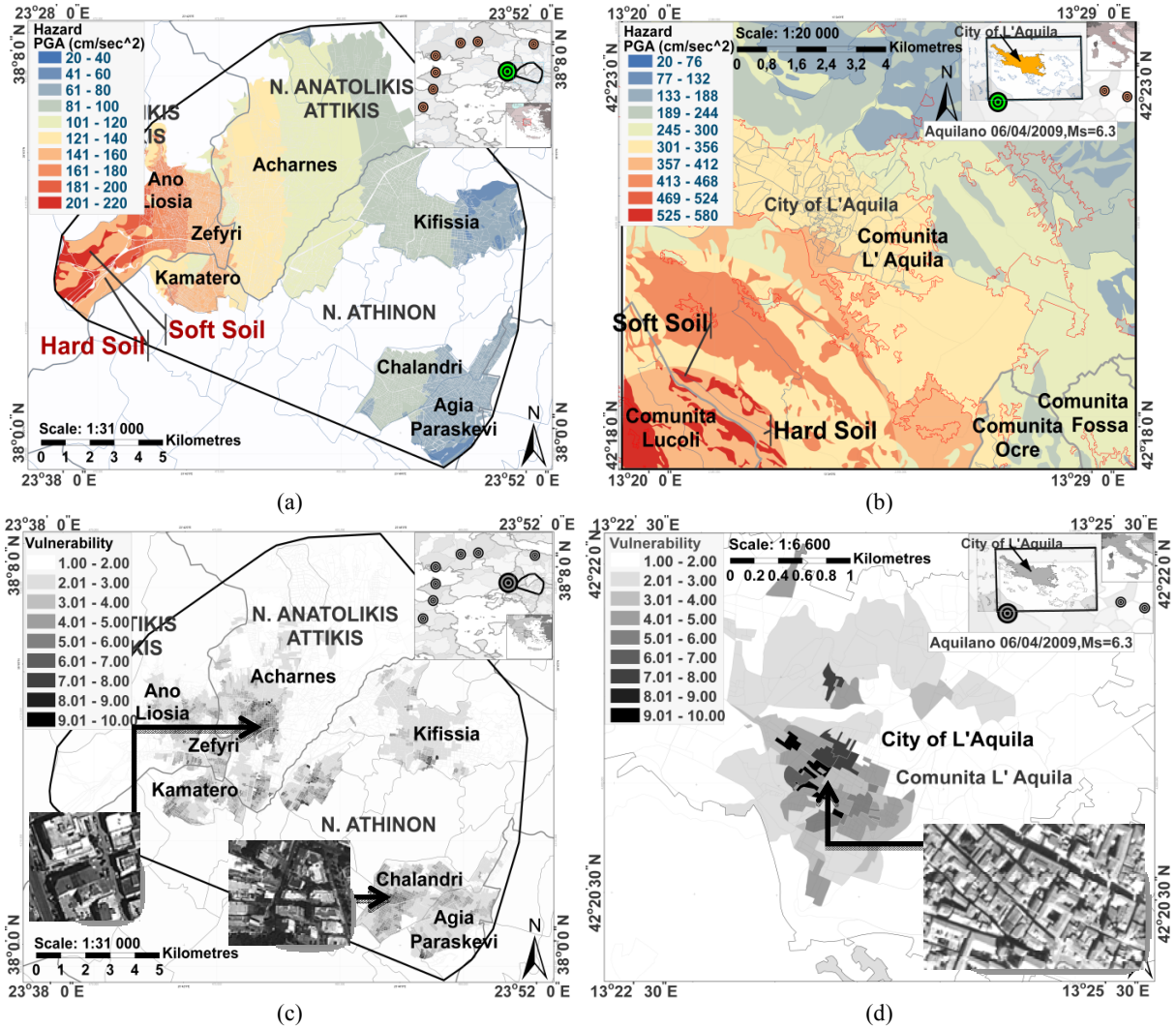

Fig. 5 Modeled hazard (PGA) for (a) the September 7, 1999 Athens earthquake scenario and (b) the April 6, 2009 L'Aquila earthquake scenario. The pattern for the PGA distribution is being controlled mainly by the epicentral distance and soil effects; Modeled building vulnerability for (c) the nine municipalities of Athens and (d) the L'Aquila city and its surroundings.

5.4 Predicted Building Damages

The normalized and relative damages obtained by running the 1999 Athens earthquake scenario are represented in Figs. 6a and 6b, respectively. From there it can be easily observed that the field of damages is consistent with the modeled PGA distribution (Fig. 5a). The highest damage is concentrated in the southwest side of the area examined, close to the seismic source and over softer soils, while the damage diminishes towards northeast. To be noted that these results conform to the damages reported on the field by the Greek Seismic Rehabilitation Agency, the so-called YAS organization, the days which followed the earthquake event. The correlation between (1) the theoretically calculated PGA values with the real PGA values recorded, as well as (2) the predicted by the model damages with the on-site recorded damages are analyzed in the validation section. At first glance the results show that the damages are controlled mainly by the features as the ground motion, namely the PGA, the geographic distribution of the underlying soils and the buildings vulnerability (Figs. 6a and 6c). The resulted normalized and relative damages, for the 2009 earthquake of L'Aquila, are presented in Figs. 6c and 6d, respectively. As in the case of Athens both the returned normalized and relative damages are higher in the southeast side of the area examined, and are locally depended on soil conditions and vulnerability. A decrease of both is observed towards northeast that is moving away from the earthquake source.

5.5 Uncontrolled Evacuation

Fig. 7 shows the results of the modeled risk due to uncontrolled evacuation of the population for one of the studied municipalities of Athens, namely Aghia Paraskevi. Conceptually, the map is a discrete surface defined only along the network. Because nearby road segments are often in the same spatial evacuation vulnerability class, groups of segments organize themselves into perceivable vulnerability clusters as evident in Fig. 7. These clusters are called evacuation sheds. The thematic map unit is the number of people per lane in a road segment's worst-case evacuation. The color corresponds to the ratio of population evacuated to the number of lanes leading out of the evacuated neighborhood, namely the BLD (bulk lane demand). Orange color represents a load of 300 persons per lane while red to more than 500. A number of "hot spots" were identified in the case of Athens. In total 15 areas spread over the nine studied municipalities of Athens, returned a BLD > 500. It has to be stressed that the greater evacuation problem was returned at the most densely populated areas of the city of Athens, where more than 70 risky neighborhoods were identified. In Fig. 7, the most risky clusters of the Municipality of Aghia Paraskevi are identified, and satellite views of them are presented. The neighborhoods denoted as A, B and C in the figure are adjacent to an open space and vehicles evacuating, although trapped, will not face an immediate risk of injury. On the other hand, in areas as D, which is a densely built-up area, the passengers in trapped vehicles are under great risk.

6. Validation of Results

6.1 Seismic Hazard

A first validation step comprised the comparison of the instrumentally recorded PGA values with the ones obtained by the MASSIVE models. The recorded PGA values were taken from local seismic networks (source: NOA-Geodynamics Institute (GR), for the Athens test site, and Instituto Nazionale di Geofisica e Vulcanologia (IT)), for the L'Aquila test site), and the relevant literature [28]. The results of correlation are illustrated in Figs. 8a and 8b and Figs. 8c and 8d for the Athens and L'Aquila test sites, respectively.

The correlation figures are considered adequate for both experiments, given the relatively small number of observations and the uncertainties involved in the

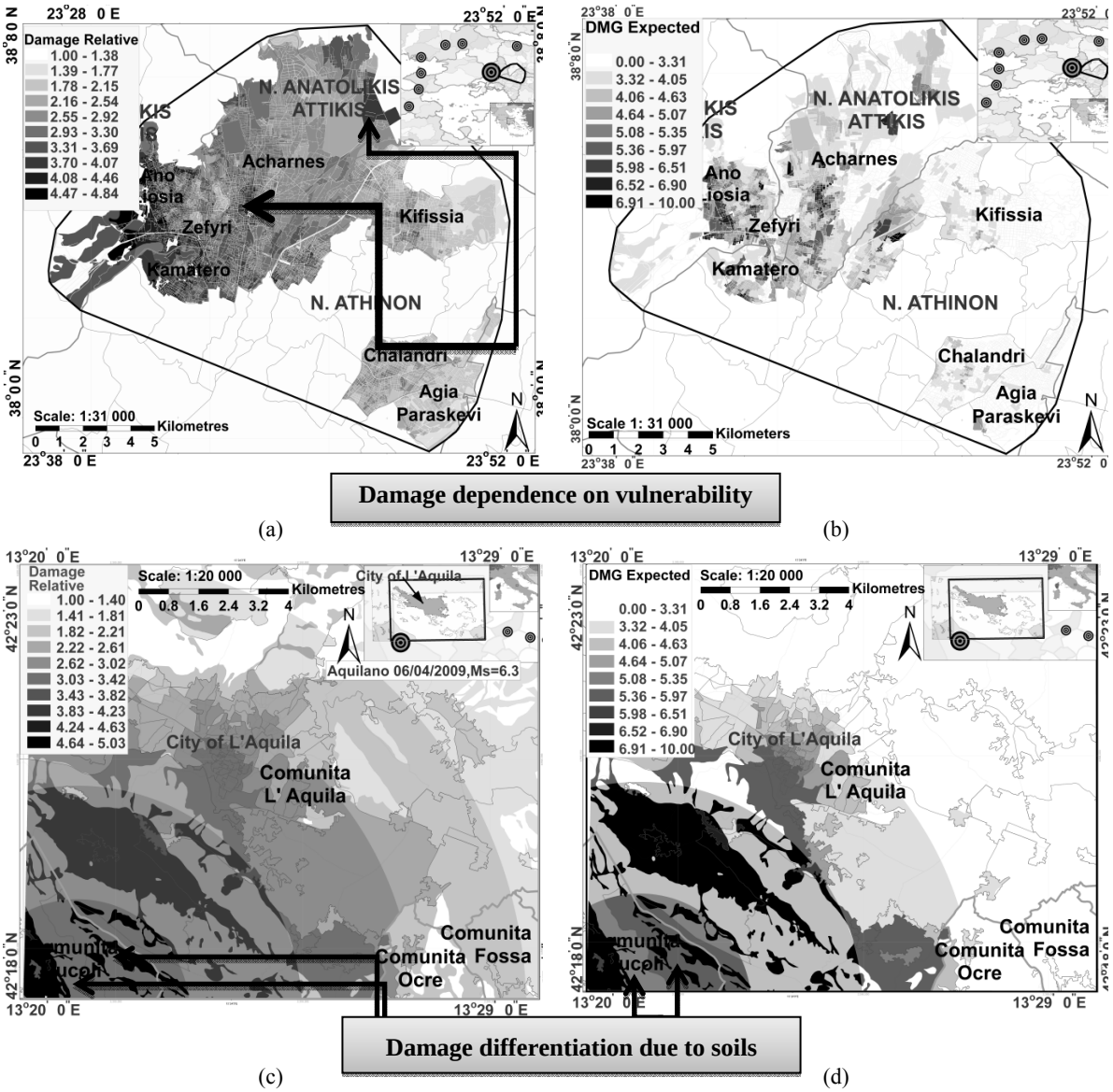

Fig. 6 (a) Relative and (b) normalized damages, relating to the 1999 Athens earthquake scenario; (c) Relative and (d) normalized damages, relating to the 2009 L'Aquila earthquake scenario.

calculation of PGA. Indeed the correlation coefficient for the test site of Athens is of the order of 0.78 while for L'Aquila is as high as 0.94. It is also of particular interest to examine and interpret the fluctuations between the on-site observed and the modeled PGA values against the corresponding epicentral distances shown in Figs. 8b and 8c. It is clear that the observed values in the near-field are higher than the modeled ones. This could be attributed to the strong energy directivity effect recognized in the rupture process for both earthquake events. Such a type of effect, however, is not incorporated in the empirical laws of PGA attenuation used in MASSIVE. As a result, the modeled values are not as high as the observed ones in the near-field domain. On the other hand, in medium-field and far-field domains the seismic energy directivity effect is not as strong as in the near-field domain and then no high discrepancies are observed. In general, the model performed better in the case of L'Aquila than in the case of Athens earthquake, returning not only higher correlation coefficients but also smaller discrepancies in the PGA

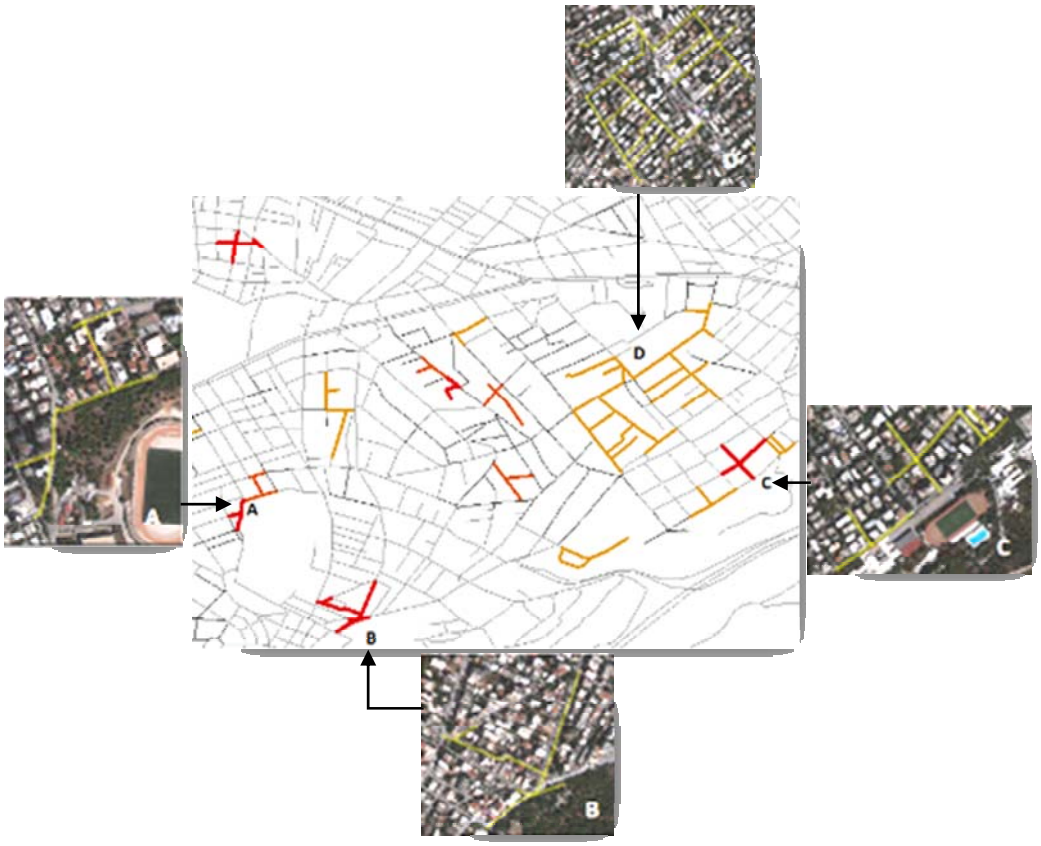

Fig. 7 An evacuation vulnerability example over the municipality of Aghia Paraskeviof Athens. The color corresponds to the ratio of population evacuated to the BLD (bulk lane demand). Orange color represents a value of 300 persons per lane while red to more than 500.

values between the modeled and the observed ones as moving away from the epicenter.

6.2 Seismic Damage

The predicted damages over the test area of Athens were validated, using as input the on-site recorded building damages provided by the Greek Seismic Rehabilitation Agency, the so-called YAS organization. The results of the field reporting works were obtained in terms of the 3-scale damage state definition, which is the common Green-Yellow-Red post earthquake tagging approach used in Greece, with the "Red tag" indicating the heavily damaged buildings, the "Yellow tag" representing the moderately damaged buildings, and the "Green tag" indicating buildings with no structural damages.

The records of the YAS database were first cleaned from inconsistencies. Then based on the building's address the Green-Yellow-Red tags were appropriately geo-located at the level of the building block. To be noted that the buildings' geo-location was successfully done for the 92% of the YAS database records, thus corresponding to a number of 2,808 "Red", 4,888 "Yellow", and 12,846 "Green" buildings.

Then, for each building block a DS (damage state) was generated by using the following formula:

$$DS = a \times Nb_{ND} + b \times Nb_G + c \times Nb_Y + d \times Nb_R \quad (11)$$

with Nb_{ND} denoting the number of the totally unaffected by the earthquake buildings, and Nb_G, Nb_Y, and Nb_R, being the affected buildings which were attributed the tags of "Green", "Yellow", and "Red"

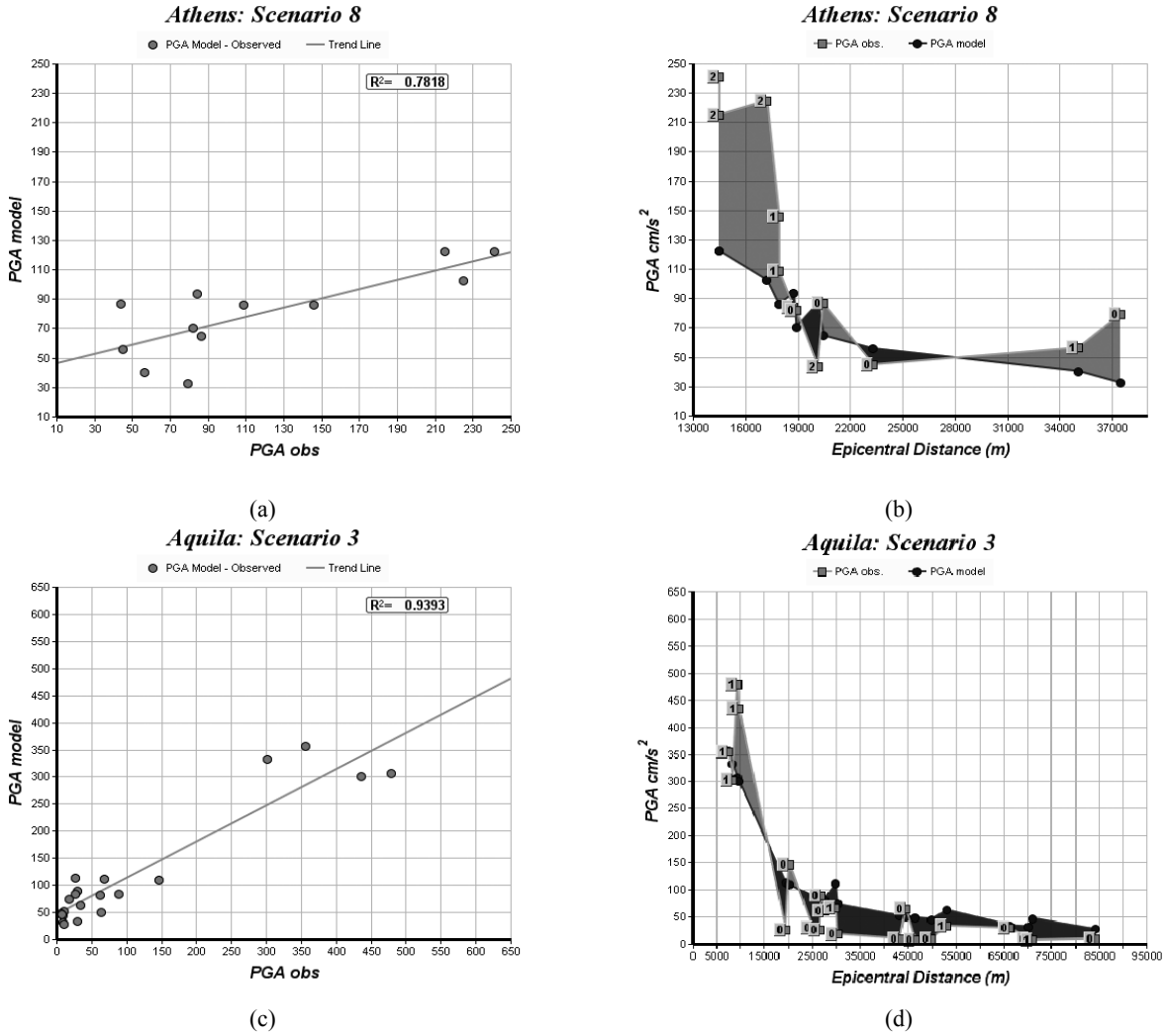

Fig. 8 Plots (a) and (c) represent the correlation between the on-site recorded versus the modeled PGA values, while plots (b) and (d) illustrate the fluctuation of PGA values with the epicenter distance, for the scenarios of Athens, and L'Aquila earthquakes, respectively.

respectively, after the field inspections of YAS. The factors *a*, *b*, *c*, and *d* are weighting factors, which have been heuristically defined as, $a = 1.0$, $b = 1.5$, $c = 2.0$, and $d = 2.5$. The calculated DS figures were normalized in the range of 1-10, and by this, the reference validation map of Fig. 9b was generated. By this, the validation of the theoretically obtained damages using MASSIVE was possible by cross-correlating the reference map of Fig. 9b above with the modeled damages of map in Fig. 9a. The obtained correlation between the two data sets was of the order of 0.80 (Fig. 10), which is considered a good fit given the very detailed scale of mapping, and the simplification assumptions in the modeling of vulnerability and hazard.

It is also interesting to see how the correlation between the modeled and the on-site reported damages changes away from the epicenter. The analysis of the returned correlation coefficients along transects N1 and N2 and S1-S3 of Fig. 11 show that they are turned to increased values with the distance from the hanging wall of the fault. Indeed the obtained values along transects S1 and N1, that are located very close to the main fault, are 0.7428 and 0.8425 respectively. The correlation values are increased to 0.8406 and 0.8769 along transects, S2 and S3, that are

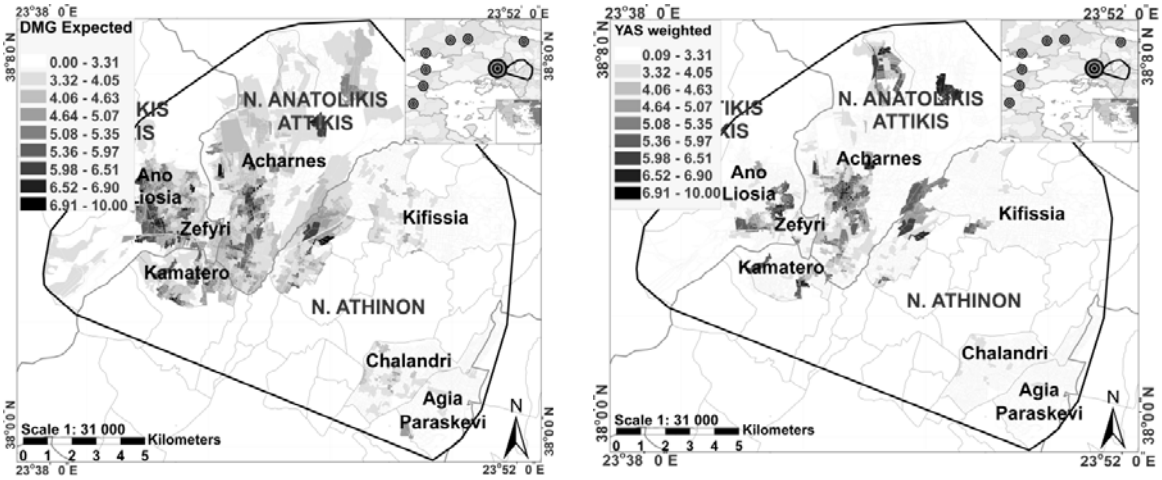

(a) (b)

Fig. 9 (a) Modeled building damages versus (b) on-site reported ones using the Green-Yellow-Red tagging scheme.

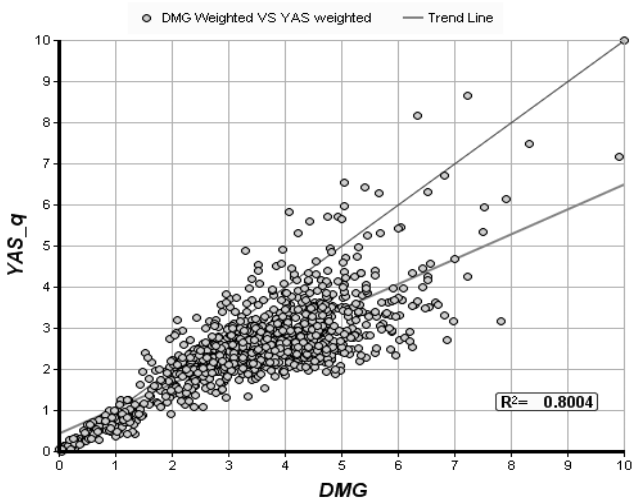

Fig. 10 Correlation between modeled and on-site reported damages over the Athens test site at building block level.

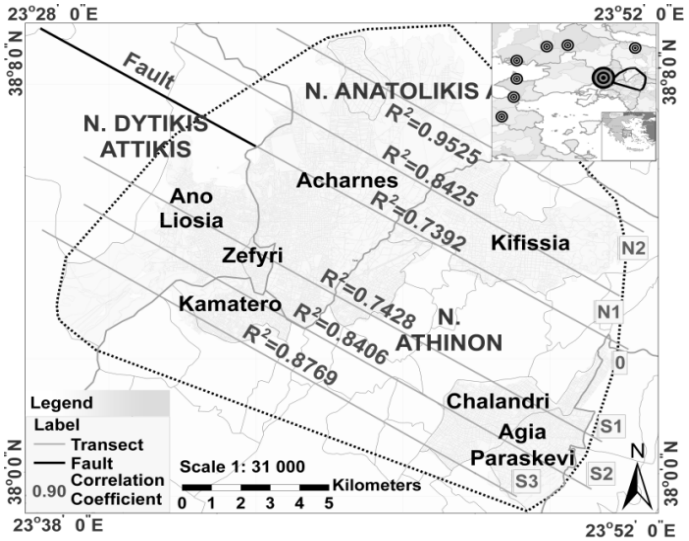

Fig. 11 Definition of transects parallel to the hanging wall of the fault along with the coefficient correlation assessments between the modeled and the on-site reported damages by YAS.

located further to the south of the main fault, as well as to 0.9525 along the transect N2 which is located further to the north of the main fault. Finally, the obtained correlation figures were significantly higher when larger geographic units that were formed by the aggregation of the building blocks were considered. In this specific case the correlation achieved between the modeled and the on-site reported damages has been as high as 0.93.

7. Discussion

MASSIVE is a geo-information environment that enables Civil Protection Organizations and Local Authorities to easily derive assessments which are useful for the establishment of large scale risk plans at city level. MASSIVE focuses on the implementation of a rather generic but at the same time reliable methodology. It exploits easily accessible information representative to soil types, population density, built up area density, and building oldness. Such data are usually found as official statistics in the archives of Geological and/or Mapping Agencies of the studied territories. Moreover, data relating to transportation network, past seismicity records, cadastral data, as well as building block geometries, can become available today over the web as open linked data. Despite the rather generic and simplified design adopted by MASSIVE, the results have been considered promising. The validation using past earthquake records returned a correlation between the modeled and the on-site measured PGAs higher than 0.75, while the correlation between the on-site reported damages versus the modeled ones were of the order of 0.80 at the detailed level of the building block. This shows that the parameters mostly affecting the level of the disaster that are the seismic hazard, and the vulnerability have been realistically approximated using the empirical formulas of MASSIVE. The study of Eqs. (2), (3) and (4), together with the resulted maps of Figs. 5 and 7, indicate that the different soil types and specifically the distinction between hard and soft soils, has been critical for the returned seismic hazard and the corresponding prediction of damages. Indeed, looking at Fig. 7, it is evident that near to the earthquake's epicenter, the level of the predicted disaster may vary significantly, with the underlying soils being the key parameter affecting this variation. Moreover, looking at Fig. 10b, one can easily observe that a similar disaster variation has been reported on the field, verifying that the level of damage followed exactly the hard/soft soil distribution pattern over the study area. By consequence the finer and more accurate the input soil data are, the more reliable the predicted damages are expected to be with MASSIVE. The same principle applies to the vulnerability parameter as well. However, it is to interesting to underline here that the simplified approximation of the vulnerability parameter used in authors' experiments, which was based solely on the oldness of the buildings, it worked well and returned acceptable and reliable assessments. It is well evident that the use of more sophisticated engineering approaches for expressing the building vulnerability based on the structural elements and the typologies of the buildings may potentially return better results. However, to achieve this, very detailed and accurate structural information on the building stock is required. For the purposes of completeness it is outlined here that this civil engineering approach was also developed and tested in the framework of MASSIVE, and the relevant GIS tools have become available, enabling the users to calculate the expected damages according to a "hybrid" method, which combines the earthquake hazard with the results of an inelastic analyses of representative structures, making thus use of the so-called fragility curves for specific building typologies [2-4]. The results of this study in MASSIVE have been the subject of a separate publication, which has been evaluated and accepted for presentation in the 15th World Conference on Earthquake Engineering at Lisbon [30]. In general, the results of both methods (simplified approximation v.s.

civil engineering one) were similar as far as the predicted damages were concerned. In general, authors faced great difficulty in applying the pure civil engineering method as described in Ref. [30], and this due to lack of representative information concerning the typology and the structural characteristics of the buildings at the level of the building bloc in both test sites. Usually, such data are not systematically collected over the urban areas, and require very intensive on-site works to acquire them. This limitation renders the proposed simplified approach much promising specially for large scale applications worldwide.

8. Conclusions

From the above it can be inferred that MASSIVE provides a prosperous methodology for approximating the expected earthquake damages in urban agglomerations. In the usual case MASSIVE implements a simplified approach acknowledging how critical is for the users to, (1) access easily the input data to run the models, and (2) to use a standardized and transferable methodology for deriving comparable assessments over the locations it applies. MASSIVE in its concept is a user oriented GIS system. For this it has been designed to run by practicing engineers and civil protection specialists without special pre-requisites and skills in GIS. It allows deriving fast assessments for any earthquake scenario, supporting the training of users and the adoption of appropriate civil protection prevention plans over urban areas that are prone to seismic and population evacuation risks. The results of the validation study are regarded with confidence for using the proposed system as a training and prevention tool.

Acknowledgments

The authors acknowledge the financial support of the Civil Protection Financial Instrument of the European Community (GRANT AGREEMENT No. 070401/2009/540429/SUB/A4). The sole responsibility of this publication lies with the authors and the Commission is not responsible for any use that may be made of the information herein.

References

[1] G.M. Calvi, R. Pinho, G. Magenes, J.J. Bommer, L.F. Restrepo-Vélez, H. Crowley, Development of seismic vulnerability assessment methodologies over the past 30 years, ISET Journal of Earthquake Technology 43 (3) (2006) 75-104.

[2] A.J. Kappos, K.C. Stylianidis, K. Pitilakis, Development of seismic risk scenarios based on a hybrid method of vulnerability assessment, Natural Hazards 17 (2) (1998) 177-192.

[3] A.J. Kappos, G. Panagopoulos, C. Panagiotopoulos, G. Penelis, A hybrid method for the vulnerability assessment of R/C and URM buildings, Bulletin of Earthquake Engineering 4 (4) (2006) 391-413.

[4] A.J. Kappos, V. Lekidis, G. Panagopoulos, I. Sous, N. Theodulidis, Ch. Karakostas, et al., Analytical estimation of economic loss for buildings in the area struck by the 1999 Athens earthquake and comparison with statistical repair costs, Earthquake Spectra 23 (2) (2007) 333-355.

[5] HAZUS, Earthquake Loss Estimation Methodology: Technical Manual, Report prepared for the Federal Emergency Management Agency by the National Institute of Building Sciences of United States, Washington, D.C., 1999.

[6] P. Mouroux, B. Lebrun, RISK-UE project: An advanced approach to earthquake risk scenarios with application to different European towns, in: C.S. Oliveira, A. Roca, X. Goula (Eds.), Assessing and Managing Earthquake Risk, Springer, Berlin, 2006, pp. 479-508.

[7] RADIUS, Risk Assessment Tools for Diagnosis of Urban Areas Against Seismic Disasters [Online], 2000, www.eird.org/eng/revista/No2_2001/pagina21.htm. (accessed June 11, 2012)

[8] S. Anagnostopoulos, C. Providakis, P. Salvaneschi, G. Athanasopoulos, G. Bonacina, SEISMOCARE: An efficient GIS tool for scenario-type investigations of seismic risk of existing cities, Soil Dynamics and Earthquake Engineering 28 (2008) 73-84.

[9] T.R. Eguchi, D.J. Goltz, A.H. Seligson, J.P. Flores, C.N. Blais, H.T. Heaton, et al., Real-time loss estimation as an emergency response decision support system: The early post-earthquake damage assessment tool (EPEDAT), Earthquake Spectra 13 (4) (1997) 815-833.

[10] P. Gueguen, C.L. Mitchel, L. Le Corre, A simplified approach for vulnerability assessment in moderate-to-low seismic hazard regions: Application to Grenoble (France), Bulletin of Earthquake Engineering 5 (3) (2007) 467-490.

[11] LESSLOSS, Risk Mitigation for Earthquakes and Landslides, Earthquake Disaster Scenario Prediction and Loss Modeling for Urban Areas LESSLOSS Report No. 2007/07, 2007.

[12] RMS, RiskLink Software and Service Brochure [Online], 2008, http://www.rms.com/Publications/RiskLink.pdf (accessed June 11, 2012). (Electronic brochure)

[13] A.G. Hobeika, B. Jamei, MASSVAC: A model for calculating evacuation times under natural disasters, Emergency Planning 15 (1985) 23-28.

[14] F. Southworth, Regional Evacuation Modeling: A State-of-the-Art Review, Oak Ridge National Laboratory ORNL-11740, Tennessee, 1991.

[15] U.J. Dymon, N.L. Winter, Evacuation mapping: The utility of guidelines, Disasters 17 (1993) 12-24.

[16] G.A. Papadopoulos, A. Arvanitides, Earthquake risk assessment in Greece, in: V. Schenk (Ed.), Earthquake Hazard and Risk, Advances in Natural & Technological Hazards Research, Kluwer Academy Publishers, 1996, pp. 221-229.

[17] A.A. Skarlatoudis, C.B. Papazachos, B.N. Margaris, N. Theodulidis, Ch. Papaioannou, I. Kalogeras, et al., Empirical peak ground-motion predictive relations for shallow earthquakes in Greece, Bull. Seismol. Soc. Am. 93 (2003) 2591-2603.

[18] F. Sabetta, A. Pugliese, Attenuation of peak horizontal acceleration and velocity from Italian strong-motion records, Bull. Seismol. Soc. Am. 77 (1987) 1491-1511.

[19] P.K. Koliopoulos, B.N. Margaris, N.S. Klimis, Duration and energy characteristics of Greek strong motion records, J. Earth Eng. 2 (1998) 391-417.

[20] L. Faenza, A. Michelini, Regression analysis of MCS intensity and ground motion parameters in Italy and its application in shake map, Geophysical Journal International 180 (2010) 1138-1152.

[21] J.H. Sorensen, B.M. Vogt, D. Mileti, Evacuation: An Assessment of Planning and Research, Oak Ridge National Laboratory ORNL-6376, Tennessee, 1987.

[22] S. Tufekci, T.M. Kisko, Regional evacuation modelling system REMS: A decision support system for emergency area evacuations, Computers and Industrial Engineering 21 (1991) 89-93.

[23] M.K. Lindell, R.W. Perry, Understanding evacuation behavior: An editorial introduction, International Journal of Mass Emergencies and Disasters 9 (1991) 133-136.

[24] Z. Sinuany-Stern, E. Stern, Simulating the evacuation of a small city: The effects of traffic factors, Socio-Economic Planning Sciences 27 (1993) 97-108.

[25] T.J. Cova, R.L. Church, Modelling community evacuation vulnerability using GIS, International Journal of Geographical Information Science 11 (1997) 763-784.

[26] A.N. Anastasiadis, M. Demosthenous, C.H. Karakostas, N. Klimis, B. Lekidis, B. Margaris, et al., The Athens (Greece) Earthquake of September 7, 1999: Preliminary Report on Strong Motion Data and Structural Response [Online], http://mceer.buffalo.edu/research/Reconnaissance/greece 9-7-99 (accessed June 2, 2012).

[27] C.C. Kontoes, P. Elias, O. Sykioti, P. Briole, D. Remy, M. Sachpazi, et al., Displacement field mapping and fault modeling of the September 7th, 1999 Athens earthquake based on ERS-2 satellite radar interferometry, Geophysical Research Letters 27 (24) (2000) 3989-3992.

[28] G.A. Papadopoulos, G. Drakatos, D. Papanastassiou, I. Kalogeras, G. Stavrakakis, Preliminary results about the catastrophic earthquake of 7 September 1999 in Athens, Greece, Seismol. Res. Lett. 71 (2000) 318-329.

[29] S. Pavlides, A. Ganas, G.A. Papadopoulos, The fault that caused the Athens September 1999 M 5.9 earthquake: Field observations, Natural Hazards 27 (2002) 61-84.

[30] Ch. Karakostas, V. Lekidis, A. Kappos, G. Panagopoulos, Ch. Kontoes, I. Keramitsoglou, Evaluation of seismic vulnerability of buildings in Athens and L'Aquila in the framework of the MASSIVE seismic mitigation system, in: Proceedings on 15th World Conference on Earthquake Engineering, Lisbon, Portugal, 2012.